2016

Improving atmospheric CO_2 retrievals using line mixing and speed-dependence when fitting high-resolution ground-based solar spectra

Joseph Mendonca
University of Toronto

Kimberly Strong
University of Toronto, strong@atmosp.physics.utoronto.ca

Geoffrey Toon
California Institute of Technology

Debra Wunch
California Institute of Technology, dwunch@caltech.edu

K Sung
California Institute of Technology

See next page for additional authors

Publication Details

Mendonca, J., Strong, K., Toon, G. C., Wunch, D., Sung, K., Deutscher, N. M., Griffith, D. W. T. & Franklin, J. E. (2016). Improving atmospheric CO_2 retrievals using line mixing and speed-dependence when fitting high-resolution ground-based solar spectra. Journal of Molecular Spectroscopy, 323 15-22.

Improving atmospheric CO_2 retrievals using line mixing and speed-dependence when fitting high-resolution ground-based solar spectra

Abstract

A quadratic speed-dependent Voigt spectral line shape with line mixing (qSDV + LM) has been included in atmospheric trace-gas retrievals to improve the accuracy of the calculated CO2 absorption coefficients. CO2 laboratory spectra were used to validate absorption coefficient calculations for three bands: the strong 20013 ← 00001 band centered at 4850 cm−1, and the weak 30013 ← 00001 and 30012 ← 00001 bands centered at 6220 cm−1 and 6340 cm−1 respectively, and referred to below as bands 1 and 2. Several different line lists were tested. Laboratory spectra were best reproduced for the strong CO2 band when using HITRAN 2008 spectroscopic data with air-broadened widths divided by 0.985, self-broadened widths divided by 0.978, line mixing coefficients calculated using the exponential power gap (EPG) law, and a speed-dependent parameter of 0.11 used for all lines. For the weak CO2 bands, laboratory spectra were best reproduced using spectroscopic parameters from the studies by Devi et al. in 2007 coupled with line mixing coefficients calculated using the EPG law. A total of 132,598 high-resolution ground-based solar absorption spectra were fitted using qSDV + LM to calculate CO2 absorption coefficients and compared to fits that used the Voigt line shape. For the strong CO2 band, the average root mean square (RMS) residual is 0.49 ± 0.22% when using qSDV + LM to calculate the absorption coefficients. This is an improvement over the results with the Voigt line shape, which had an average RMS residual of 0.60 ± 0.21%. When using the qSDV + LM to fit the two weak CO2 bands, the average RMS residual is 0.47 ± 0.19% and 0.51 ± 0.20% for bands 1 and 2, respectively. These values are identical to those obtained with the Voigt line shape. Finally, we find that using the qSDV + LM decreases the airmass dependence of the column averaged dry air mole fraction of CO2 retrieved from the strong and both weak CO2 bands when compared to the retrievals obtained using the Voigt line shape.

Disciplines

Medicine and Health Sciences | Social and Behavioral Sciences

Publication Details

Mendonca, J., Strong, K., Toon, G. C., Wunch, D., Sung, K., Deutscher, N. M., Griffith, D. W. T. & Franklin, J. E. (2016). Improving atmospheric CO_2 retrievals using line mixing and speed-dependence when fitting high-resolution ground-based solar spectra. Journal of Molecular Spectroscopy, 323 15-22.

Authors

Joseph Mendonca, Kimberly Strong, Geoffrey Toon, Debra Wunch, K Sung, Nicholas M. Deutscher, David W. T Griffith, and J E. Franklin

Improving atmospheric CO_2 retrievals using line mixing and speed-dependence when fitting high-resolution ground-based solar spectra

Authors: J. Mendonca[1], K. Strong[1], G.C. Toon[3], D. Wunch[2], K. Sung[3], N. M. Deutscher[4], D.W.T. Griffith[4], and J.E. Franklin[5].

1. Department of Physics, University of Toronto, Toronto, ON, CA

2. California Institute of Technology, Pasadena, CA, USA

3. Jet Propulsion Laboratory, California Institute of Technology, Pasadena, CA, USA

4. Center for Atmospheric Chemistry, University of Wollongong, Wollongong, NSW, Australia

5. Department of Physics and atmospheric Science, Dalhousie University, Halifax, NS, CA

Correspondence to: J. Mendonca (joseph.mendonca@utoronto.ca)

Address: 60 St. George Street, Toronto, ON, M5S 1A7

Abstract

A quadratic speed-dependent Voigt spectral line shape with line mixing (qSDV+LM) has been included in atmospheric trace-gas retrievals to improve the accuracy of the calculated CO_2 absorption coefficients. CO_2 laboratory spectra were used to validate absorption coefficient calculations for three bands: the strong 20013<-00001 band centered at 4850 cm^{-1}, and the weak 30013<-00001 and 30012<-00001 bands centered at 6220 cm^{-1} and 6340 cm^{-1} respectively, and referred to below as bands 1 and 2. Several different line lists were tested. Laboratory spectra were best reproduced for the strong CO_2 band when using HITRAN 2008 spectroscopic data with air-broadened widths divided by 0.985, self-broadened widths divided by 0.978, line mixing coefficients calculated using the Exponential Power Gap (EPG) law, and a speed-dependent parameter of 0.11 used for all lines. For the weak CO_2 bands, laboratory spectra were best reproduced using spectroscopic parameters from the studies by Devi et al. in 2007 coupled with line mixing coefficients calculated using the EPG law. A total of 132,598 high-resolution ground-based solar absorption spectra were fitted using qSDV+LM to calculate CO_2 absorption coefficients and compared to fits that used the Voigt line shape. For the strong CO_2 band, the average root mean square

(RMS) residual is 0.49 ± 0.22% when using qSDV+LM to calculate the absorption coefficients. This is an improvement over the results with the Voigt line shape, which had an average RMS residual of 0.60 ± 0.21%. When using the qSDV+LM to fit the two weak CO_2 bands, the average RMS residual is 0.47 ± 0.19% and 0.51 ± 0.20% for bands 1 and 2, respectively. These values are identical to those obtained with the Voigt line shape. Finally, we find that using the qSDV+LM decreases the airmass dependence of the column averaged dry air mole fraction of CO_2 retrieved from the strong and both weak CO_2 bands when compared to the retrievals obtained using the Voigt line shape.

Key words: CO_2, Absorption coefficient, Line mixing, Speed-dependence, high-resolution solar spectra

1. Introduction

The increasing global-averaged land-surface temperature has been attributed to the rise in radiative forcing due to increasing concentration of greenhouse gases (GHGs). There has been a 7.5% increase in radiative forcing from well-mixed GHGs from 2005-2011 with 80% of this increase due to CO_2, making it the most important anthropogenic GHG [1]. Sources and sinks of CO_2 are located near the Earth's surface, with their location and strength derived from *in situ* measurements. The density of *in situ* sites is relatively high over North America and Europe while low over South America, Africa, and the oceans. To determine the global distribution of CO_2, space-based measurements of reflected sunlight have been made by SCIAMACHY from 2002 to 2012 [2], the Japanese Greenhouse gases Observing SATellite (GOSAT) from 2009 to the present [3], and NASA's Orbiting Carbon Observatory (OCO-2) from 2014 to the present [4]. GOSAT and OCO-2 use the strong 20013<-00001 CO_2 band centered at 4850 cm^{-1} and the weak 30013<-00001 CO_2 band (referred to as "band 1" below) centered at 6220 cm^{-1}) [3] [4] while SCIAMACHY uses the weak 30012<-00001 band centered at 6340 cm^{-1} (referred to as "band 2" below) along with another band to retrieve total columns of CO_2. High-resolution ground-based solar

absorption spectra from the Total Carbon Column Observing Network [5] are used to validate the space-based measurements with total columns of CO_2 retrieved using both weak CO_2 bands.

For CO_2 measurements from space to be useful for carbon cycle studies, they must be made with an accuracy better than 1 ppm [6] [7]. This requires high-precision spectroscopy with accurate spectral line shapes for calculating CO_2 absorption coefficients [8]–[12]. Laboratory studies of CO_2 spectroscopic parameters and spectral line shapes [8]–[12] assert that the Voigt spectral line shape is insufficient for modeling the spectral line shape of CO_2 to attain the necessary precision and accuracy for carbon cycle studies. These studies claim that speed-dependence, collisional narrowing, and line mixing need to be taken into account when calculating absorption coefficients for both weak CO_2 bands. Hartmann et al. [13] used two days of direct sun solar absorption spectra, recorded with a Fourier transform spectrometer at Park Falls (Wisconsin, USA), using absorption coefficients calculated with a Voigt line shape with line mixing. Total columns of CO_2 were retrieved using the strong CO_2 band and the weak CO_2 band. The authors showed that taking line mixing into account improved spectral fits and decreased the airmass dependence of the dry-air mole fraction (XCO_2) for both bands, with the greatest impact on the strong CO_2 band. Hartmann et al. [13] further showed that the airmass dependence of XCO_2 retrieved with a Voigt spectral line shape is not geophysical in nature due to the inadequacy of the Voigt spectral line shape. If this is not taken into account, it could lead to incorrect inferences about regional sources and sinks.

Thompson et al. [14] compared the performance of absorption coefficients calculated with the software of Lamouroux et al. [15] with that of the OCO-2 approach for taking both line mixing and speed-dependence into account. Validation of these absorption coefficients was done by simulating laboratory spectra for the measurement conditions and fitting high-resolution ground-based solar absorption

spectra. By taking into account both speed-dependence and line mixing, fits to solar absorption spectra were improved and the airmass dependence of XCO_2 decreased.

The goals of this study are: (1) to show that using the quadratic speed-dependent Voigt (qSDV) spectral line shape of Tran et al. [16] with first-order line mixing coefficients and temperature dependence calculated using the exponential power gap law is a viable approach for calculating CO_2 absorption coefficients, and (2) to assess the impact this has on retrievals of CO_2 total column amounts. To accomplish this we test several spectral line lists (developed using line shapes described by Voigt, Voigt with line mixing, or speed-dependent Voigt with line mixing) by evaluating their ability to reproduce high-resolution laboratory spectra under a variety of conditions. We then fit high-resolution solar absorption spectra taking into account speed-dependence and line mixing in the absorption coefficient calculations. Section 2 of this study provides a review of the spectral line shapes. A description of how first-order line mixing coefficients are calculated for a temperature range of 250-350 K is described in Section 3. Laboratory spectra are used to assess the calculation of CO_2 absorption coefficients in Section 4. Finally, in Section 5, solar spectra recorded at four TCCON stations are fitted using a Voigt and qSDV line shape with line mixing (qSDV+LM). The quality of the spectral fits is assessed along with the resulting impact on the XCO_2 airmass dependence.

2. Spectral Line Shapes

The CO_2 absorption coefficients are calculated using different spectral line shapes and spectroscopic parameters and compared to determine the best combination. This section describes how absorption coefficients are calculated, taking into account pressure broadening, Doppler broadening, speed-dependence, and line mixing.

2.1 Line Mixing

Line mixing occurs when the difference between rotational energy levels within the same vibrational level is smaller than the thermal energy. This allows inelastic collisions to transfer population from one rotational level to another [17]. The absorption coefficient for lines that are coupled can be calculated using the equation [18]:

$$k(v) = \frac{1}{\pi} Im\left\{\vec{\boldsymbol{\mu}}^T \cdot \left[v\boldsymbol{I} - \boldsymbol{v_o} - iP\boldsymbol{W}\right]^{-1} \cdot \boldsymbol{\rho} \cdot \vec{\boldsymbol{\mu}}\right\} \quad (1)$$

where k is the absorption coefficient at a given frequency v, $\vec{\boldsymbol{\mu}}$ is a column vector of the transition dipole moments, P is the pressure, $\boldsymbol{\gamma}$ is a diagonal matrix of Lorentz widths, $\boldsymbol{v_o}$ is a diagonal matrix of line centers, $\boldsymbol{\rho}$ is a diagonal matrix of lower state populations for each transition, $\boldsymbol{W}$ is the relaxation matrix describing the coupling of spectral lines, and $\boldsymbol{I}$ is the identity matrix. The diagonal elements of $\boldsymbol{W}$ are Lorentz widths and the off-diagonal elements are the collisional transfer rate ϵ_{jk}, which represents the transfer of population from lower rotational level k to higher rotational level j. For a molecule in thermodynamic equilibrium, the rate of upward transfer is related to the rate of downward transfer through the detailed balance condition:

$$\rho_k \epsilon_{jk} = \rho_j \epsilon_{kj} \quad (2)$$

where ρ_k is the population of rotational level k and ρ_j is the population of rotational level j [11]. The off-diagonal elements of $\boldsymbol{W}$ are related to the diagonal elements of $\boldsymbol{W}$ through the sum rule, resulting in the equation:

$$W_{kk} = \gamma_k = \frac{1}{2}\left[\sum_{j \neq k} \epsilon_{jk}\right]_{Upper} + \frac{1}{2}\left[\sum_{j \neq k} \epsilon_{jk}\right]_{Lower} \quad (3)$$

where $Upper$ denotes the upper vibrational level and $Lower$ denotes the lower vibrational level as stated in Ref. [11].

The ϵ_{jk} for CO_2 can be modeled using the exponential power gap (EPG) law [18]:

$$\epsilon_{jk} = a_1 \left[\frac{\Delta E_{jk}}{k_B T}\right]^{-a_2} e^{\left(\frac{-a_3 \Delta E_{jk}}{k_B T}\right)} \tag{4}$$

where ΔE_{jk} is the difference between rotational energy levels j and k, k_B is the Boltzmann constant, T is the temperature, and a_1, a_2, and a_3 are coefficients that need to be determined (refer to section 3 for details on how they are calculated). Once the coefficients are determined, the EPG law is used to calculate the off-diagonal elements of $\boldsymbol{W}$ using the equation:

$$W_{\substack{jk \\ j \neq k}} = -\beta \epsilon_{jk} \tag{5}$$

where $\beta = 0.56$ is the parity bias [11].

For lines that weakly overlap, the Rozenkranz first-order approximation [19] can be used to simplify Eq. 1, resulting in the absorption coefficient for the aysmmetrical Voigt line shape:

$$k(v) = \frac{1}{\pi} \sum_i \frac{S_i \left(P\gamma^i + PY^i \left(v - v_o^i - P\delta_o^i\right)\right)}{\left(v - v_o^i - P\delta_o^i\right)^2 + \left(\gamma^i\right)^2} \tag{6}$$

where S_i is the intensity of spectral line, , δ_o^i is the pressure shift and Y^i is the line mixing coefficient. The latter is calculated using [17]:

$$Y^i = 2 \sum_{j \neq i} \frac{\mu_j}{\mu_i} \frac{W_{ji}}{v_i - v_j}, \tag{7}$$

and the Lorentz width, γ^i, varies according to the equation:

$$\gamma^i (T) = \mathrm{P} \times \gamma_o^i \left(\frac{296}{T}\right)^n \tag{8}$$

where T is the temperature, and n is the exponent of temperature dependence. When Y^i equals zero in Eq. 6 this leads to the Lorentz line shape.

2.2 Voigt with Line Mixing

For retrievals from atmospheric spectra, it is necessary to take both pressure broadening and Doppler broadening into account. Convolving the Doppler profile with Eq. 6 [17] results in the absorption coefficient using the asymmetric Voigt line shape (or Voigt with line mixing):

$$k(v) = \frac{1}{\pi}\sum_i S_i \left(\frac{1}{\gamma_{D_i}}\right)\left(\frac{\ln(2)}{\pi}\right)^{1/2} \left(Re[c(v, x_i, y_i)] + PY^i\, Im[c(v, x_i, y_i)]\right) \quad (9)$$

where

$$x_i = \frac{\left(v - v_o^i \quad - P\delta_o^i\right)}{\gamma_{D_i}}(\ln(2))^{1/2}, \qquad y_i = \frac{\gamma^i}{\gamma_{D_i}}(\ln(2))^{1/2} \quad (10)$$

γ_{D_i} is the Doppler width at a given temperature, and c is the complex probability function. Setting Y^i to zero in Eq. 9 would result in absorption coefficients calculated with a Voigt line shape.

2.3 Speed-Dependent Voigt with Line Mixing

Speed-dependence arises when the collision speed between the absorbing and perturbing molecules cannot be adequately described by just the mean speed of the Maxwellian speed distribution. Both the Lorentz width and shift will vary depending on the speed of collision. These are calculated by the formula given in [20]:

$$\gamma^i\,(\mathrm{v}) = \mathrm{P} \times\, \gamma_o^i(1 + a_\gamma^i((\mathrm{v})^2 - 1.5)), \qquad \delta_o^i(\mathrm{v}) = \mathrm{P} \times \delta_o^i(1 + a_\delta^i((\mathrm{v})^2 - 1.5)), \quad (11)$$

where v is the ratio of the speed of the absorbing molecule to its most probable speed, a_γ^i is the speed-dependent Lorentz parameter and a_δ^i is the speed-dependent pressure shift parameter. This creates a

Lorentz profile for each speed that is averaged over a Maxwellian velocity distribution. The absorption coefficients calculated using a speed-dependent Voigt line shape with line mixing are given by:

$$k(v) = \left(\frac{2}{\pi^{\frac{3}{2}}}\right)\sum_i S_i \int_{-\infty}^{\infty} e^{-\mathrm{v}^2}\mathrm{v}\left(tan^{-1}\left[\frac{x_i+\mathrm{v}}{y_i}\right] + PY^i\,\frac{1}{2}ln\left[\left(\frac{x_i+\mathrm{v}}{y_i}\right)^2+1\right]\right)dv \quad (12)$$

with δ_o^i replaced with $\delta_o^i(\mathrm{v})$ in x_i and γ^i replaced with $\gamma^i(\mathrm{v})$ in y_i and all other terms as defined above. To enhance computational efficiency, the quadratic-speed-dependent Voigt (qSDV) from Ref. [16] was used to calculate absorption coefficients when using the speed-dependent Voigt with line mixing spectral line shape.

3. Calculating the Line Mixing Coefficient

The line mixing coefficient for a given CO_2 band is calculated using the EPG law (Eq. 4) to model the rate of transfer between rotational levels. In order to use Eq. 4, the a_1, a_2, and a_3 coefficients need to be determined. When constructing $\boldsymbol{W}$, the columns of the matrix should sum to zero (Eq. 3). Substituting Eq. 4 into Eq. 3 and also taking detailed balance into account (Eq. 2) results in an over-determined system of equations, with n equations (where n is the number of spectral lines), and three unknowns. The coefficients a_1, a_2, and a_3 are determined by solving the system of non-linear equations using the Levenberg-Marquardt algorithm. It should be noted that we assume only coupling between lines in the same branch, following Ref. [10]. Once a_1, a_2, and a_3 are determined, all off-diagonal elements of $\boldsymbol{W}$ are calculated by substituting Eq. 4 into Eq. 5. Eq. 7 is then used to determine the line mixing coefficient for each line.

Given that the Lorentz width changes with temperature (Eq. 8), the line mixing coefficient will also have a temperature dependence. The line mixing coefficient of each line was thus calculated for a temperature range between 250-350 K at 2 K intervals. Figure 1 shows the line mixing coefficient

plotted as a function of $\left(\frac{296}{T}\right)$, for the P(24) spectral line of the weak CO_2 band 1. A quadratic line is fitted to the data showing that Y^i can be accurately modeled by a quadratic equation, similar to Ref. [17], making it easy to use in any retrieval algorithm:

$$Y^i\,(T) = a_i\left(\frac{296}{T}\right)^2 + b_i\left(\frac{296}{T}\right) + c_i \tag{13}$$

where a_i, b_i, and c_i are the coefficients for line i determined by fitting a quadratic line to the $Y^i\,(T)$ data. The coefficients a_i, b_i, and c_i are then stored in a list with the other spectroscopic parameters for line i so that Y^i can be easily calculated using Eq. 13. However, the calculated $Y^i\,(T)$ will be different for collisions of CO_2 with air, it self and H_2O. To adequately take into account all types of collisions, the total line mixing coefficient $Y^i_{total}(T)$ for a given line will be calculated using:

$$Y^i_{total}(T) = \chi_{air}.Y^i_{air}(T) + \chi_{self}.Y^i_{self}(T) + \chi_{H2O}.Y^i_{H2O}(T) \tag{14}$$

where χ is the dry air mole fraction of the collision partner (air, self or H_2O), $Y^i_{air}(T)$, $Y^i_{self}(T)$, and $Y^i_{H2O}(T)$ are the line mixing coefficients calculated for the different collision partners and modeled by Eq. 13. We assume that the Lorentz widths from collisions with H_2O are 1.35 times the air-broadened widths. So when calculating $Y^i_{H2O}(T)$, the air-broadened Lorentz widths are increased 35% to calculate the rate of transfer between rotational levels. In order to calculate $Y^i_{total}(T)$, there will be nine parameters for each CO_2 line. Given Eq. 11, the Lorentz width is not only a function of T but also v, when speed-dependence is taken into account. Ref. [21] shows that there is negligible difference between using a speed-dependent and speed-independent line mixing coefficient. So in this study, Y^i is simply a function of T when speed-dependence is taken into account in the spectral line shape.

4. Fitting Laboratory Spectra

To assess the absorption coefficients calculated for CO_2 using the spectral line shapes described in Section 2 for both the strong and weak CO_2 bands, spectra calculated using the GFIT retrieval program [5] [22] were compared to laboratory spectra recorded at known laboratory conditions (temperature, humidity) and known CO_2 amounts in a temperature-controlled absorption cell with an optical path length of 29.30 m. The absorption coefficients were calculated using spectroscopic parameters from different laboratory studies that retrieved the parameters using three spectral line shapes: Voigt (Eq. 9 with $Y^i = 0$), Voigt with line mixing (Eq. 9), and speed-dependent Voigt with line mixing (qSDV from Tran et al. 2013). The line mixing coefficients for a given set of spectroscopic parameters were calculated as described in Section 3. The different spectral line shapes were compared and the best spectral line shape was chosen as the new standard to calculate CO_2 absorption coefficients when fitting solar spectra based on the ability to model laboratory spectra.

4.1 Fitting a CO_2 Laboratory Spectrum for the Strong CO_2 Band

For the strong CO_2 band, a laboratory spectrum was recorded at the Jet Propulsion Laboratory (JPL) using a Bruker 125HR Fourier transform spectrometer (FTS) at a resolution of 0.0044 cm^{-1}. The cell contained a total gas pressure of 0.7892 atm at 296.1 K with 4.96% being ^{12}C-enriched $^{16}O^{12}C^{16}O$ [14]. Figure 2a shows the measured laboratory spectrum. The forward model contained in the GGG software suite [5,22] was used to simulate the measured spectrum by calculating the absorption coefficients using three different line shapes: (1) a Voigt, (2) Voigt with line mixing, and (3) quadratic speed-dependent Voigt with line mixing (qSDV+LM). The spectroscopic parameters used to calculate the absorption coefficients with the different spectral line shapes are from HITRAN 2008 [23] and HITRAN 2012 [24]. How the HITRAN 2008 and HITRAN 2012 spectroscopic parameters were modified for appropriate use with the qSDV+LM will be explained later in this section. It should be noted that the different spectral line shapes were only used to calculate the absorption coefficients for CO_2 lines for the

strong CO_2 band. Absorption coefficients for all other spectral lines were calculated assuming a Voigt line shape and spectroscopic parameters from the default spectral line list, atm.101 [25], which is provided with the GGG software package [5,22]. The atm.101 line list [25] is a combination of spectroscopic parameters from HITRAN and other studies that use a Voigt spectral line shape when calculating absorption coefficients. The assumption we make about all other CO_2 lines in this window is adequate because the strengths of the CO_2 lines in the strong CO_2 band are approximately 15 times greater than the other CO_2 lines, and including speed-dependence and line mixing for these weak lines had no effect on the quality of the spectral fits.

Figures 2b and 2c show the residuals (measured minus calculated spectrum) for absorption coefficients calculated using a Voigt line shape and spectroscopic parameters from HITRAN 2008 (Figure 2a) and HITRAN 2012 (Figure 2b). The overall fit, given by the RMS (root mean square) residual, is slightly better when using the HITRAN 2012 spectroscopic parameters. However, both residuals show the same systematic structure. Figures 3a and 3c are plots of the P-branch residuals from 4832.5-4836.6 cm^{-1} and Figures 3b and 3d show the R-branch residuals from 4870-4874 cm^{-1} using a Voigt line shape with HITRAN 2008 and HITRAN 2012, respectively. These residuals clearly show an asymmetric structure regardless of the spectroscopic parameters used to calculate the absorption coefficients.

Figures 2d and e show the residuals for absorption coefficients calculated using a Voigt line shape that includes line mixing with HITRAN 2008 (Figure 2d) and HITRAN 2012 (Figure 2e) parameters. HITRAN 2012 CO_2 Lorentz widths were calculated by adjusting intermolecular parameters from Refs. [26]–[28] to model the speed-dependent Voigt widths that were measured in Refs. [8] and [9]. Lamouroux et al. [29] has shown that the HITRAN 2012 air- and self-broadened widths need to be adjusted in order to calculate absorption coefficients with a Voigt line shape with line mixing. In this work (as well as Lamouroux et al. [29]), the adjustment was done by determining the transition-averaged ratio of Lorentz

widths measured using a Voigt line shape to the speed-dependent Voigt line shape, and then multiplying by this factor. In the studies by Predoi-Cross et al. [10] and [11], air- and self-broadened Lorentz widths were measured using the Voigt and speed-dependent Voigt line shapes. The average ratio of all the air-broadened Lorentz widths measured in Ref. [10] using a Voigt line shape to those measured using the speed-dependent Voigt line shape is 0.985 (as determined in Ref. [29]). For self- broadened Lorentz widths (measured in Ref. [11]) this ratio is 0.978 (as determined in Ref. [29]). So to convert from Voigt air-broadened Lorentz widths to speed-dependent Voigt air-broadened Lorentz widths, we divide the Voigt air-broadened Lorentz widths by 0.985 (and for self-broadened Lorentz widths we divide by 0.978). Since the HITRAN 2012 Lorentz widths represent speed-dependent air- and self-broadened Lorentz widths [29], we want to convert from speed-dependent Voigt to speed-independent Voigt so we multiply the air- and self-broadened widths by 0.985 and 0.978, respectively. Figure 2e shows the residual obtained with the adjusted HITRAN 2012 widths and a Voigt with line mixing. The overall spectral fit was improved for both HITRAN 2008 and HITRAN 2012, but slightly better for HITRAN 2008 than HITRAN 2012. Figures 3e and 3f shows that the asymmetry has been substantially diminished when using HITRAN 2008 with a Voigt line shape and line mixing. The result is the same for HITRAN 2012 (Figures 3g and 3h) but a "w" structure remains at line center for all the lines shown in the plots irrespective of line parameters.

Multiple laboratory studies have shown that in addition to line mixing, speed-dependence should also be taken into account [8]–[11]. To do this empirically, the same speed-dependent parameter $\alpha^i = 0.11$ was used for all lines. This is the average value of α from the measurements of Ref. [8] and [9]. We further assume that α is the same for both air- and self-broadened widths as done in Refs. [8] and [9]. In order to use HITRAN 2008 parameters with the speed-dependent Voigt line shape, the air- and self-broadened widths were multiplied by 1/0.985 and 1/0.978 respectively, while HITRAN 2012 parameters were returned to their original values.

Figures 2f and 2g show the residuals obtained using the qSDV+LM to calculate the absorption coefficients with HITRAN 2008 and HITRAN 2012 spectroscopic parameters. The overall spectral fit improved for both sets of spectroscopic parameters when speed-dependence was taken into account in addition to line mixing. Figures 3i and 3j show that the residual at line center was reduced when using qSDV+LM and the empirically scaled HITRAN 2008 spectroscopic parameters. The results were the same for HITRAN 2012 (Figures 3k and 3l), but the empirical HITRAN 2008 parameters fitted the spectrum better than the empirical HITRAN 2012 parameters. Therefore when fitting solar spectra for the strong CO_2 band, the new CO_2 absorption coefficients will be calculated using qSDV+LM and the empirically scaled HITRAN 2008 spectroscopic parameters.

4.2 Fitting a CO_2 laboratory Spectrum for the Weak CO_2 bands

In this section, the absorption coefficients are calculated using either a Voigt line shape, Voigt with line mixing, or qSDV+LM spectral line shape. The line mixing parameter is calculated, following the method of Section 3, for widths determined for the weak CO_2 bands. Absorption coefficients for all weak lines in the spectral fitting windows are calculated with a Voigt line shape and spectroscopic parameters from HITRAN 2012.

Currently, the forward model uses spectroscopic parameters from the atm.101 line list [25] for the weak CO_2 bands with a Voigt spectral line shape. These CO_2 spectroscopic parameters are an earlier version of parameters from Ref. [30] that consistently produced the best fits to multiple high-resolution solar absorption spectra recorded at multiple TCCON sites. Figures 4a and 5a show the measured spectra for both bands, recorded at JPL using a Bruker 125HR FTS at a resolution of 0.00667 cm^{-1}. The total gas pressure is 0.7892 atm at 295.3 K with 9.03% being 12C-enriched $^{16}O^{12}C^{16}O$ [14]. Figures 4b and 5b show the difference between the measured and calculated spectra, the latter using a Voigt with spectroscopic parameters from the atm.101 line list [25] for both bands. Figures 4c and 5c show the residual when a

Voigt line shape with line mixing and spectroscopic parameters from the atm.101 line list [25] are used to calculate the absorption coefficients. The overall fit (given by the RMS residual), and the systematic structure in the residual has improved as a result of including line mixing.

A series of studies by Predoi-Cross et al. on the CO_2 spectral line shape were published starting in 2007. Ref. [10] fitted laboratory spectra using both a Voigt and speed-dependent Voigt with line mixing spectral line shape. Air-broadened half-widths, pressure shifts, and line mixing coefficients were measured in this study. Line intensity, self-broadened half-widths, pressure shifts, and line mixing coefficients were measured by Ref. [11]. In both these studies, line positions and the speed-dependent parameters were taken from Ref. [8] for the weak CO_2 band 1, and Ref. [9] for the weak CO_2 band 2. The temperature dependence of air-broadened half-widths was determined in Ref. [32]. Figures 4d, 4e, and 4f show the spectral fits with a Voigt, Voigt with line mixing and qSDV+LM line shape for the weak CO_2 band 1. Figures 5d, 5e, and 5f are the same as Figure 4 but for the weak CO_2 band 2. For both weak CO_2 bands the fits get better when line mixing is used and improve further when speed-dependence is also taken into account. Including speed-dependence and line mixing with spectroscopic parameters from Ref. [10], [11], and [32] results in better fits to the laboratory spectra than the atm.101 [25] spectroscopic parameters with a Voigt line shape.

Finally, the spectrum was calculated using the spectroscopic parameters from Ref. [8] for the weak CO_2 band 1, and Ref. [9] for the weak CO_2 band 2, using qSDV+LM. The residuals of the fit are shown in Figures 5g and 6g for both windows. In this case, the fits for both windows are better than all other line shape models. Therefore when fitting solar spectra, the new absorption coefficients will be calculated using the qSDV+LM and spectroscopic parameters from Ref. [8] and [9].

5. Fitting Solar Spectra

High-resolution solar absorption interferograms used in this work were recorded at a resolution of 0.02 cm^{-1} with Bruker IFS 125HR FTS instruments located at four TCCON stations: Eureka, Canada; Park Falls, USA; Lamont, USA; and Darwin, Australia [5]. Interferograms are corrected for solar intensity variations [33], phase errors, and laser sampling errors [22]. They are then fast Fourier transformed into spectra [35]. Surface pressure, temperature and other weather data are also recorded at each site. The surface pressure measurements are used to derive the site pressure-altitude for each spectrum as described in Ref. [5]. In the spectral fitting process, the forward model uses daily *a priori* profiles for temperature, pressure, humidity, and H_2O from 6-hourly National Centers for Environmental Prediction (NCEP/NCAR) reanalysis data [36]. This is coupled with daily *a priori* profiles created by empirical models for CO_2 and other trace gases [5]. The GFIT code is used to retrieve a volume mixing ratio scale factor (VSF) that is applied to the *a priori* profile to calculate the total column amount of CO_2.

5.1 Fitting the Strong CO_2 Band

A typical Eureka (eu) [37] solar spectrum recorded at SZA 84^o on March 17, 2014 was fitted using the Voigt with HITRAN 2012 CO_2 spectroscopic parameters and qSDV+LM and the empirical HITRAN 2008 parameters for the strong CO_2 band (see Figure 6). All other spectral lines, except solar lines, were fitted using a Voigt line shape with parameters from the atm.101 line list [25]. Solar lines were calculated using the empirical solar line list [38]. Figure 6 shows two residual spectra (measured minus calculated) in the top panel, where the green line indicates the residual for the current retrieval and the blue indicates the residual taking speed-dependence and line mixing into account. The bottom panel shows the measured and calculated spectra, as well as the contribution from the various other absorbing species in this window. Taking both speed-dependence and line mixing into account reduces the structure in the residual and decreases the RMS residual, but some structure remains.

For a more robust test, solar spectra from Eureka, Park Falls (pa) [39], Lamont (oc), and Darwin (db) [40] were fitted with the qSDV+LM spectral line shape. All four sites record spectra in accordance with TCCON standards and represent a large range of atmospheric conditions (hot, cold, wet, dry, etc.). Figure 7 shows the RMS residual for the spectral fits plotted as a function of SZA. Figure 7a shows the RMS residual resulting from fitting the spectra using the Voigt spectral line shape with HITRAN 2012 parameters. Figure 7b shows the RMS residual of the spectral fits when using the qSDV+LM and the empirical HITRAN 2008 parameters. Figure 7c shows the percent difference of the RMS residual between the qSDV+LM and Voigt spectral line shapes for the different sites. The spectral fits improve as a function of SZA with the greatest improvement at SZA of 82^o with the new CO_2 absorption coefficients. Above 82^o SZA, the difference decreases as a function of SZA. The average RMS residual using a Voigt line shape is 0.60 ± 0.21% and using qSDV+LM is 0.49 ± 0.22%.

The dry air mole fraction, XCO_2, is calculated using:

$$XCO_2 = (Column\ of\ CO_2 / Column\ of\ O_2) * 0.2095 \quad (15)$$

where $Column\ of\ CO_2$ is the weighted average of the columns retrieved from both weak CO_2 bands, $Column\ of\ O_2$ is the column retrieved from the 7885 cm^{-1} window with a Voigt line shape and taking collision-induced absorption (CIA) into account [41], and 0.2095 is the assumed dry air mole fraction of O_2 in the atmosphere. Calculating XCO_2 in this way reduces errors common to both CO_2 and O_2 (e.g., solar pointing errors, small instrument line shape errors, etc.) since they are retrieved from the same spectrum in adjacent spectral regions [5].

Figure 8 shows XCO_2 retrieved using both spectral line shapes for the four sites. Figure 8a shows XCO_2 calculated using the CO_2 column retrieved with a Voigt line shape and Figure 8b shows XCO_2 calculated from the CO_2 column retrieved using qSDV+LM. Figure 8c shows the percent difference for the XCO_2 retrieved using the different spectral line shapes (($XCO_2^{qSDV+LM}$- XCO_2^{Voigt})/ XCO_2^{Voigt}). At the lowest SZA,

0.1% more CO_2 is retrieved with the new absorption coefficients with the difference decreasing until SZA of approximately 20^o where there is no difference in CO_2 between the two retrievals. Less CO_2 is retrieved using the qSDV+LM as a function of SZA (for SZA>20^o) peaking at about 2% less at SZA of 85^o. For SZA greater than 85^o, the retrieval done with the Voigt line shape retrieves less CO_2 (airmass dependence changes) and so the difference between the spectral line shapes decreases. The absolute mean percentage difference in XCO_2 retrieved using the two sets of absorption coefficients is 0.40 ± 0.42% using measurements from all sites.

5.2 Fitting the Weak CO_2 Bands

Figure 9 shows a typical spectral fit for the weak CO_2 band 1 for a measurement taken at Eureka at a SZA of 84^o. The top panel shows the residual using a Voigt line shape (red) with spectroscopic parameters from the atm.101 line list [25] and using qSDV+LM (blue) with parameters from Ref. [8]. Figure 10 shows the same spectrum but for the weak CO_2 band 2. Systematic structure seen in the Voigt residual is reduced in both windows when using the qSDV+LM spectral line shape. However, some systematic structure in the spectral fits remains.

Figures 11 and 12 are the same as Figure 7 but for the weak CO_2 bands 1 and 2 respectively. For both windows, as the SZA increases, the spectral fits are best when the qSDV+LM is used. The impact of the new absorption coefficients on the RMS residuals increases with SZA. At a SZA of 85^o, the RMS residual at Eureka decreased by 25% while at Darwin it only decreased by 5%. The mean RMS residual from all measurements for the weak CO_2 band 1 was found to be 0.47 ± 0.19%, and 0.51 ± 0.20% for the weak CO_2 band 2 when using a Voigt spectral line shape. Using the qSDV+LM, the mean RMS residual is 0.47 ± 0.20% for the weak CO_2 band 1 and 0.51 ± 0.20% for the weak CO_2 band 2. Given the change in the spectral fit, this will have an impact on the retrieved CO_2 column amount.

Figure 13 shows XCO_2 for the CO_2 column that is the weighted average of CO_2 columns retrieved from the weak CO_2 bands as a function of SZA for all four sites, in the same way as in Figure 8. At all four sites, the column of CO_2 retrieved using qSDV+LM is 0.5% greater than the Voigt retrieval at a SZA of 1^o. As the SZA increases, so does the amount of CO_2 retrieved with qSDV+LM compared to the Voigt. At 70^o SZA, the column of CO_2 retrieved with qSDV+LM is 0.6% greater compared to the Voigt retrievals. For SZA greater than 70^o, the difference between the two retrievals decreases until a SZA of approximately 85^o. Less CO_2 is retrieved with the qSDV+LM compared to the Voigt line shape for SZA greater than 85^o. The absolute mean % difference in XCO_2 retrieved using the two sets of absorption coefficients is 0.57 ± 0.09% using measurements from all sites.

To compare the two weak CO_2 bands, we look at the correlations between retrieved VSFs. Figure 14a shows the correlation between the VSFs retrieved using a Voigt spectral line shape. Figure 14b shows the correlation between the VSFs retrieved using the qSDV+LM. The line of best fit (black line) is also shown in each plot along with the correlation coefficient (r). The correlation between the weak bands is good as indicated by r, which is 0.88 for both spectral line shapes.

Discussion

Our choice of speed-dependence and line mixing scheme was shown to improve the accuracy of fits to laboratory spectra for the strong and weak CO_2 bands. We chose the EPG law to model off-diagonal relaxation matrix elements because Ref. [10] showed that it gives better results for modeling first-order line mixing coefficients than the Energy Corrected Sudden (ECS) law. Using the EPG law has two advantages: (1) we can construct the full relaxation matrix to take into account mixing between multiple lines in the branch of a band; and (2) we can calculate the temperature dependence of the first-order line mixing coefficient (shown in Section 3). Off-diagonal relaxation matrix elements from Ref. [8] and [9] were not used to constuct the relaxation matrix because the temperature dependence of these

parameters is not avaliable. Ref. [14] mentions that neglecting the temperature dependence of line mixing could be one of the sources of the remaining residual structure in their modeling of laboratory spectra of the strong and weak CO_2 bands.

We chose to use first-order line mixing instead full line mixing for two reasons: first, the studies by Ref. [10] and [11] fitted laboratory spectra using first-order line mixing, and second, to address the need to decrease the computation time for absorption coefficient calculations. To compute full line mixing requires calculation of the relaxation matrix and then diagonalization and inversion, which are computationally intensive processes. With our approach, there is no need to compute the relaxation matrix, as this is done off-line: all we need is Eq. 13 to take into account first-order line mixing for air, self, and H_2O collisions.

One of the assumptions we make when computing Lorentz widths of CO_2 is that the H_2O-broadening is 1.35 times the air-broadening. However, the study by Ref. [42] shows that it is more likely to be twice the air-broadened width for rotational quantum number (J) higher than 10. This might have a small impact on measurements made through a wet atmosphere. If a study is done to determine the H_2O-broadened Lorentz width of CO_2 for the strong and weak CO_2 bands, the first-order line mixing coefficient for collisions with H_2O can be recalculated.

The qSDV of Ref. [16] was used to take speed-dependence into account instead of the numerical integration scheme used in Ref. [14] to minimize absorption coefficient computing time. In Ref. [16] the numerical integration scheme was compared to the qSDV and the difference between calculated values was found to be on the order of 10^{-9}. When fitting solar spectra, absorption coefficients are calculated on our server at the University of Toronto. Daily absorption coefficient calculations are performed using an Intel(R) Xeon(R) CPU E5-2643 v2 @ 3.50GHz processor and takes approximately 4.5 s for a day's worth of solar spectra for the Voigt calculation for the weak CO_2 band 1. With the qSDV, the absorption

coefficient calculations take approximately 9 s, which is the result of having to do the Voigt calculation twice when calculating the qSDV.

Recently studies by Ref. [43] and [12] have shown the need to take into account Dicke (collisional) narrowing when fitting CO_2 transitions for the weak CO_2 band 1 and the strong CO_2 band respectively. Any remaining residual structure seen when modeling the laboratory spectra might be due to neglecting Dicke narrowing when calculating the absorption coefficients. Assessing the impact of including Dicke narrowing in our absorption coefficient calculations could be done when the relevant parameters for the partially-correlated quadratic speed-dependent hard collision spectral line shape of Ref. [16] for all CO_2 transitions in the strong and weak CO_2 bands become available.

Using speed-dependence and line mixing to calculate absorption coefficients in the manner described here could be beneficial for CO_2 vertical profile retrievals. Vertical profile information comes from the spectral line shape: the wings of the spectral line carry information about CO_2 near the surface and the line center has information primarily about the higher altitudes [44]. The wings of the line are sensitive to effects like line mixing, while the center of the line can be affected by speed-dependence. A spectral line shape that takes these effects into account will allow more accurate profile retrievals. Partial columns of CO_2 have been retrieved using the weak CO_2 band 1 [44], [45] the strong CO_2 band [46]. Use of the qSDV+LM should be tested with a vertical profile retrieval algorithm to assess the impact of speed-dependence and line mixing on the quality of the profile retrieval. When comparing the VSFs retrieved from the different bands, we have shown that the correlation between the weak CO_2 bands for both the Voigt line shape and qSDV+LM is the same. This is because a consistent set of spectroscopic parameters was used for both retrievals, and may also be due to their similarity in terms of strength and wavelength proximity.

There are two differences between the empirical parameters that we used for the strong CO_2 band compared to those used for the weak band. The first is that the line intensity was not changed and since the line intensity represents the integrated line absorption, the choice of spectral line shape affects the line intensity. Ref. [43] showed that the spectrum area obtained using a Voigt line shape was 2% lower than the speed-dependent Nelkin-Ghatak line shape. Since not much is known about the intensity changes between the Voigt and speed-dependent Voigt, the intensities were left unchanged. The second difference is that we used the same speed-dependent parameter for all CO_2 lines in the strong band. The studies by Ref. [8] and [9] show that the speed-dependent parameter has a J dependence. So these two differences could be why the correlation between the weak and the strong bands are so poor even when speed-dependence and line mixing are taken into account. If a study similar to Ref. [8] and [9] was done for the strong CO_2 band, it would be easy to incorporate those spectroscopic parameters into our absorption coefficient calculations to check the correlation between the VSFs retrieved between the strong and the weak bands.

In Section 5, we show that the airmass dependence of XCO_2 is different for the different spectral line shapes used for absorption coefficient calculations in the retrieval of CO_2 total columns. Currently, TCCON XCO_2 is retrieved from both weak CO_2 bands using a Voigt spectral line shape and the airmass dependence is corrected using an empirical formula detailed in Appendix A, Section (e) of Ref. [5]. This airmass dependence must be corrected, otherwise this artifact would alias into the seasonal cycle and lead to spurious biases between sites, as the mean SZA changes throughout the year and with latitude. The empirical correction works well for XCO_2 recorded up to a SZA of 82^o but fails to fit the shape of the airmass dependence for measurements taken at higher SZA (Figure 6 of Ref. [5]). Using the qSDV+LM spectral line shape, the empirical airmass correction can be extended to measurements made at SZA ≥ 82^o. This would result in more data available from all TCCON sites.

Conclusion

We have demonstrated an effective and efficient method to account for speed-dependence and line mixing when calculating absorption coefficients. The use of qSDV to take into account speed-dependence, and the EPG law to calculate first-order line mixing, was validated using laboratory spectra for the strong and weak CO_2 bands. High-resolution ground-based solar spectra were fitted and total columns of CO_2 were retrieved using a Voigt spectral line shape and using qSDV+LM. We find that including both speed-dependence and line mixing improved the quality of the fitted spectra and changed the XCO_2 airmass dependence when compared to the retrievals using the Voigt line shape. Less CO_2 was retrieved from the strong CO_2 band as a function of SZA. For the weak CO_2 bands, the quality of the fitted spectra improved and less CO_2 was retrieved using qSDV+LM compared to using the Voigt line shape for SZA greater than 70^o. When comparing VSF retrieved from the different bands, we showed that there needs to be a consistent set of spectroscopic parameters for absorption coefficient calculations so that the difference in VSF retrieved for the different bands is reduced. The scheme to take both line mixing and speed-dependence into account proposed in this study can be easily implemented into a retrieval algorithm in order to improve the quality of spectral fits for both the strong and weak CO_2 bands.

Acknowledgements

This work was primarily supported by the Canadian Space Agency (CSA) and the Natural Sciences and Engineering Research Council of Canada (NSERC). The Eureka measurements were made at the Polar Environment Atmospheric Research Laboratory (PEARL) by the Canadian Network for the Detection of Atmospheric Change (CANDAC), which has been supported by the AIF/NSRIT, CFI, CFCAS, CSA, Environment Canada (EC), Government of Canada IPY funding, NSERC, OIT, ORF, PCSP, and FQRNT. The authors wish to thank the staff at EC's Eureka Weather Station and CANDAC for the logistical and on-site

support provided. Thanks to CANDAC Principal Investigator James R. Drummond, PEARL Site Manager Pierre Fogal, and CANDAC/PEARL operators Mike Maurice and Peter McGovern, for their invaluable assistance in maintaining and operating the Bruker 125HR. We thank Paul O. Wennberg for making available solar absorption spectra from Park Falls and Lamont. Geoff C. Toon, Debra Wunch, and Paul O. Wennberg acknowledge support from NASA for the development of TCCON via grant number NNX14AI60G. We thank Linda Brown and Chris Benner for making available laboratory measurements of CO_2. Part of the research was performed at the Jet Propulsion Laboratory, California Institute of Technology, under contract with the National Aeronautics and Space Administration. Darwin TCCON measurements are possible thanks to support from NASA grants NAG5-12247 and NNG05-GD07G and the Australian Research Council grants DP140101552, DP110103118, DP0879468 and LP0562346. We are grateful to the DOE ARM program for technical support in Darwin. Nicholas Deutscher is supported by an ARC-DECRA DE140100178.

Bibliography

[1] Field, C.B., V.R. Barros, D.J. Dokken, K.J. Mach, M.D. Mastrandrea, T.E. Bilir, M. Chatterjee, K.L. Ebi, Y.O. Estrada, R.C. Genova, B. Girma, E.S. Kissel, A.N. Levy, S. MacCracken, P.R. Mastrandrea, and L.L. White, "IPCC, 2014: Climate Change 2014: Impacts, Adaptation, and Vulnerability. Part A: Global and Sectoral Aspects. Contribution of Working Group II to the Fifth Assessment Report of the Intergovernmental Panel on Climate Change," Cambridge University Press, Cambridge, United Kingdom and New York, NY, USA.

[2] M. Buchwitz, S. Noël, K. Bramstedt, V. V. Rozanov, M. Eisinger, H. Bovensmann, S. Tsvetkova, and J. P. Burrows, "Retrieval of trace gas vertical columns from SCIAMACHY/ENVISAT near-infrared nadir spectra: first preliminary results," *Adv. Space Res.*, vol. 34, no. 4, pp. 809–814, 2004.

[3] T. Yokota, Y. Yoshida, N. Eguchi, Y. Ota, T. Tanaka, H. Watanabe, and S. Maksyutov, "Global Concentrations of CO_2 and CH_4 Retrieved from GOSAT: First Preliminary Results," *Sola*, vol. 5, pp. 160–163, 2009.

[4] D. Crisp, R. M. Atlas, F.-M. Breon, L. R. Brown, J. P. Burrows, P. Ciais, B. J. Connor, S. C. Doney, I. Y. Fung, D. J. Jacob, C. E. Miller, D. O'Brien, S. Pawson, J. T. Randerson, P. Rayner, R. J. Salawitch, S. P. Sander, B. Sen, G. L. Stephens, P. P. Tans, G. C. Toon, P. O. Wennberg, S. C. Wofsy, Y. L. Yung, Z. Kuang, B. Chudasama, G. Sprague, B. Weiss, R. Pollock, D. Kenyon, and S. Schroll, "The Orbiting Carbon Observatory (OCO) mission," *Adv. Space Res.*, vol. 34, no. 4, pp. 700–709, 2004.

[5] D. Wunch, G. C. Toon, J.-F. L. Blavier, R. A. Washenfelder, J. Notholt, B. J. Connor, D. W. T. Griffith, V. Sherlock, and P. O. Wennberg, "The Total Carbon Column Observing Network," *Philos. Trans. R. Soc. Math. Phys. Eng. Sci.*, vol. 369, no. 1943, pp. 2087–2112, May 2011.

[6] P. J. Rayner and D. M. O'Brien, "The utility of remotely sensed CO_2 concentration data in surface source inversions," *Geophys. Res. Lett.*, vol. 28, no. 1, pp. 175–178, Jan. 2001.
[7] C. E. Miller, D. Crisp, P. L. DeCola, S. C. Olsen, J. T. Randerson, A. M. Michalak, A. Alkhaled, P. Rayner, D. J. Jacob, P. Suntharalingam, D. B. A. Jones, A. S. Denning, M. E. Nicholls, S. C. Doney, S. Pawson, H. Boesch, B. J. Connor, I. Y. Fung, D. O'Brien, R. J. Salawitch, S. P. Sander, B. Sen, P. Tans, G. C. Toon, P. O. Wennberg, S. C. Wofsy, Y. L. Yung, and R. M. Law, "Precision requirements for space-based data," *J. Geophys. Res. Atmospheres*, vol. 112, no. D10, p. D10314, May 2007.
[8] V. M. Devi, D. C. Benner, L. R. Brown, C. E. Miller, and R. A. Toth, "Line mixing and speed dependence in CO_2 at 6227.9 cm^{-1}: Constrained multispectrum analysis of intensities and line shapes in the 30013 ← 00001 band," *J. Mol. Spectrosc.*, vol. 245, no. 1, pp. 52–80, Sep. 2007.
[9] V. Malathy Devi, D. C. Benner, L. R. Brown, C. E. Miller, and R. A. Toth, "Line mixing and speed dependence in CO_2 at 6348 cm^{-1}: Positions, intensities, and air- and self-broadening derived with constrained multispectrum analysis," *J. Mol. Spectrosc.*, vol. 242, no. 2, pp. 90–117, Apr. 2007.
[10] A. Predoi-Cross, W. Liu, C. Holladay, A. V. Unni, I. Schofield, A. R. W. McKellar, and D. Hurtmans, "Line profile study of transitions in the 30012 ← 00001 and 30013 ← 00001 bands of carbon dioxide perturbed by air," *J. Mol. Spectrosc.*, vol. 246, no. 1, pp. 98–112, Nov. 2007.
[11] A. Predoi-Cross, A. V. Unni, W. Liu, I. Schofield, C. Holladay, A. R. W. McKellar, and D. Hurtmans, "Line shape parameters measurement and computations for self-broadened carbon dioxide transitions in the 30012 ← 00001 and 30013 ← 00001 bands, line mixing, and speed dependence," *J. Mol. Spectrosc.*, vol. 245, no. 1, pp. 34–51, Sep. 2007.
[12] T. Q. Bui, D. A. Long, A. Cygan, V. T. Sironneau, D. W. Hogan, P. M. Rupasinghe, R. Ciuryło, D. Lisak, and M. Okumura, "Observations of Dicke narrowing and speed dependence in air-broadened CO_2 lineshapes near 2.06 μm," *J. Chem. Phys.*, vol. 141, no. 17, p. 174301, Nov. 2014.
[13] J.-M. Hartmann, H. Tran, and G. C. Toon, "Influence of line mixing on the retrievals of atmospheric CO_2 from spectra in the 1.6 and 2.1 μm regions," *Atmos Chem Phys*, vol. 9, no. 19, pp. 7303–7312, Oct. 2009.
[14] D. R. Thompson, D. Chris Benner, L. R. Brown, D. Crisp, V. Malathy Devi, Y. Jiang, V. Natraj, F. Oyafuso, K. Sung, D. Wunch, R. Castaño, and C. E. Miller, "Atmospheric validation of high accuracy CO_2 absorption coefficients for the OCO-2 mission," *J. Quant. Spectrosc. Radiat. Transf.*, vol. 113, no. 17, pp. 2265–2276, Nov. 2012.
[15] J. Lamouroux, H. Tran, A. L. Laraia, R. R. Gamache, L. S. Rothman, I. E. Gordon, and J.-M. Hartmann, "Updated database plus software for line-mixing in CO2 infrared spectra and their test using laboratory spectra in the 1.5–2.3 μm region," *J. Quant. Spectrosc. Radiat. Transf.*, vol. 111, no. 15, pp. 2321–2331, Oct. 2010.
[16] H. Tran, N. H. Ngo, and J.-M. Hartmann, "Efficient computation of some speed-dependent isolated line profiles," *J. Quant. Spectrosc. Radiat. Transf.*, vol. 129, pp. 199–203, Nov. 2013.
[17] D. P. Edwards and L. L. Strow, "Spectral line shape considerations for limb temperature sounders," *J. Geophys. Res. Atmospheres*, vol. 96, no. D11, pp. 20859–20868, Nov. 1991.
[18] B. Gentry and L. L. Strow, "Line mixing in a N_2-broadened CO_2 Q branch observed with a tunable diode laser," *J. Chem. Phys.*, vol. 86, no. 10, pp. 5722–5730, May 1987.
[19] P. W. Rosenkranz, "Shape of the 5 mm oxygen band in the atmosphere," *IEEE Trans. Antennas Propag.*, vol. 23, no. 4, pp. 498–506, Jul. 1975.
[20] F. Rohart, H. Mäder, and H.-W. Nicolaisen, "Speed dependence of rotational relaxation induced by foreign gas collisions: Studies on CH_3F by millimeter wave coherent transients," *J. Chem. Phys.*, vol. 101, no. 8, pp. 6475–6486, Oct. 1994.
[21] R. Berman, *Direct measurements of line mixing, line broadening, and: translational line shape in the V_1+V_2 Q-branch of pure CO2.* |c[1998], 1998.

[22] Wunch, D., G. C. Toon, V. Sherlock, N. M. Deutscher, X. Liu, D. G. Feist, and P. O. Wennberg. The Total Carbon Column Observing Network's GGG2014 Data Version. doi:10.14291/tccon.ggg2014.documentation.R0/ 1221662, 2015.

[23] L. S. Rothman, I. E. Gordon, A. Barbe, D. C. Benner, P. F. Bernath, M. Birk, V. Boudon, L. R. Brown, A. Campargue, J.-P. Champion, K. Chance, L. H. Coudert, V. Dana, V. M. Devi, S. Fally, J.-M. Flaud, R. R. Gamache, A. Goldman, D. Jacquemart, I. Kleiner, N. Lacome, W. J. Lafferty, J.-Y. Mandin, S. T. Massie, S. N. Mikhailenko, C. E. Miller, N. Moazzen-Ahmadi, O. V. Naumenko, A. V. Nikitin, J. Orphal, V. I. Perevalov, A. Perrin, A. Predoi-Cross, C. P. Rinsland, M. Rotger, M. Šimečková, M. A. H. Smith, K. Sung, S. A. Tashkun, J. Tennyson, R. A. Toth, A. C. Vandaele, and J. Vander Auwera, "The HITRAN 2008 molecular spectroscopic database," *J. Quant. Spectrosc. Radiat. Transf.*, vol. 110, no. 9–10, pp. 533–572, Jun. 2009.

[24] L. S. Rothman, I. E. Gordon, Y. Babikov, A. Barbe, D. Chris Benner, P. F. Bernath, M. Birk, L. Bizzocchi, V. Boudon, L. R. Brown, A. Campargue, K. Chance, E. A. Cohen, L. H. Coudert, V. M. Devi, B. J. Drouin, A. Fayt, J.-M. Flaud, R. R. Gamache, J. J. Harrison, J.-M. Hartmann, C. Hill, J. T. Hodges, D. Jacquemart, A. Jolly, J. Lamouroux, R. J. Le Roy, G. Li, D. A. Long, O. M. Lyulin, C. J. Mackie, S. T. Massie, S. Mikhailenko, H. S. P. Müller, O. V. Naumenko, A. V. Nikitin, J. Orphal, V. Perevalov, A. Perrin, E. R. Polovtseva, C. Richard, M. A. H. Smith, E. Starikova, K. Sung, S. Tashkun, J. Tennyson, G. C. Toon, V. G. Tyuterev, and G. Wagner, "The HITRAN2012 molecular spectroscopic database," *J. Quant. Spectrosc. Radiat. Transf.*, vol. 130, pp. 4–50, Nov. 2013.

[25] Toon, G. C., "Telluric line list for GGG2014, TCCON data archive," *Carbon Dioxide Inf. Anal. Cent. Oak Ridge Natl. Lab. Oak Ridge Tenn. USA*, doi: 10.14291/tccon.ggg2014.atm.R0/1221656.

[26] R. R. Gamache and J. Lamouroux, "Predicting accurate line shape parameters for CO_2 transitions," *J. Quant. Spectrosc. Radiat. Transf.*, vol. 130, pp. 158–171, Nov. 2013.

[27] J. Lamouroux, R. R. Gamache, A. L. Laraia, J.-M. Hartmann, and C. Boulet, "Semiclassical calculations of half-widths and line shifts for transitions in the 30012←00001 and 30013←00001 bands of CO_2 II: Collisions with O_2 and air," *J. Quant. Spectrosc. Radiat. Transf.*, vol. 113, no. 11, pp. 991–1003, Jul. 2012.

[28] J. Lamouroux, R. R. Gamache, A. L. Laraia, J.-M. Hartmann, and C. Boulet, "Semiclassical calculations of half-widths and line shifts for transitions in the 30012←00001 and 30013←00001 bands of CO_2. III: Self collisions," *J. Quant. Spectrosc. Radiat. Transf.*, vol. 113, no. 12, pp. 1536–1546, Aug. 2012.

[29] J. Lamouroux, L. Régalia, X. Thomas, J. Vander Auwera, R. R. Gamache, and J.-M. Hartmann, "CO_2 line-mixing database and software update and its tests in the 2.1 μm and 4.3 μm regions," *J. Quant. Spectrosc. Radiat. Transf.*, vol. 151, pp. 88–96, Jan. 2015.

[30] R. A. Toth, L. R. Brown, C. E. Miller, V. Malathy Devi, and D. C. Benner, "Spectroscopic database of CO_2 line parameters: 4300–7000 cm^{-1}," *J. Quant. Spectrosc. Radiat. Transf.*, vol. 109, no. 6, pp. 906–921, Apr. 2008.

[32] A. Predoi-Cross, A. R. W. McKellar, D. C. Benner, V. M. Devi, R. R. Gamache, C. E. Miller, R. A. Toth, and L. R. Brown, "Temperature dependences for air-broadened Lorentz half-width and pressure shift coefficients in the 30013←00001 and 30012←00001 bands of CO_2 near 1600 nm This article is part of a Special Issue on Spectroscopy at the University of New Brunswick in honour of Colan Linton and Ron Lees.," *Can. J. Phys.*, vol. 87, no. 5, pp. 517–535, May 2009.

[33] G. Keppel-Aleks, G. C. Toon, P. O. Wennberg, and N. M. Deutscher, "Reducing the impact of source brightness fluctuations on spectra obtained by Fourier-transform spectrometry," *Appl. Opt.*, vol. 46, no. 21, p. 4774, 2007.

[34] L. Mertz, "Auxiliary computation for Fourier spectrometry," *Infrared Phys.*, vol. 7, no. 1, pp. 17–23, Mar. 1967.

[35] G. Bergland, “A radix-eight fast Fourier transform subroutine for real-valued series,” *IEEE Trans. Audio Electroacoustics*, vol. 17, no. 2, pp. 138–144, Jun. 1969.
[36] E. Kalnay, M. Kanamitsu, R. Kistler, W. Collins, D. Deaven, L. Gandin, M. Iredell, S. Saha, G. White, J. Woollen, Y. Zhu, A. Leetmaa, R. Reynolds, M. Chelliah, W. Ebisuzaki, W. Higgins, J. Janowiak, K. C. Mo, C. Ropelewski, J. Wang, R. Jenne, and D. Joseph, “The NCEP/NCAR 40-Year Reanalysis Project,” *Bull. Am. Meteorol. Soc.*, vol. 77, no. 3, pp. 437–471, Mar. 1996.
[37] R. L. Batchelor, K. Strong, R. Lindenmaier, R. L. Mittermeier, H. Fast, J. R. Drummond, and P. F. Fogal, “A New Bruker IFS 125HR FTIR Spectrometer for the Polar Environment Atmospheric Research Laboratory at Eureka, Nunavut, Canada: Measurements and Comparison with the Existing Bomem DA8 Spectrometer,” *J. Atmospheric Ocean. Technol.*, vol. 26, no. 7, pp. 1328–1340, Jul. 2009.
[38] Toon, G. C., “Solar line list for GGG2014,” *TCCON Data Arch. Hosted Carbon Dioxide Inf. Anal. Cent. Oak Ridge Natl. Lab. Oak Ridge Tenn. USA*, doi: 10.14291/tccon.ggg2014.atm.R0/1221656.
[39] R. A. Washenfelder, G. C. Toon, J.-F. Blavier, Z. Yang, N. T. Allen, P. O. Wennberg, S. A. Vay, D. M. Matross, and B. C. Daube, “Carbon dioxide column abundances at the Wisconsin Tall Tower site,” *J. Geophys. Res. Atmospheres*, vol. 111, no. D22, p. D22305, Nov. 2006.
[40] N. M. Deutscher, D. W. T. Griffith, G. W. Bryant, P. O. Wennberg, G. C. Toon, R. A. Washenfelder, G. Keppel-Aleks, D. Wunch, Y. Yavin, N. T. Allen, J.-F. Blavier, R. Jiménez, B. C. Daube, A. V. Bright, D. M. Matross, S. C. Wofsy, and S. Park, “Total column CO_2 measurements at Darwin, Australia – site description and calibration against in situ aircraft profiles,” *Atmos Meas Tech*, vol. 3, no. 4, pp. 947–958, Jul. 2010.
[41] I. E. Gordon, S. Kassi, A. Campargue, and G. C. Toon, “First identification of the electric quadrupole transitions of oxygen in solar and laboratory spectra,” *J. Quant. Spectrosc. Radiat. Transf.*, vol. 111, no. 9, pp. 1174–1183, Jun. 2010.
[42] K. Sung, L. R. Brown, R. A. Toth, and T. J. Crawford, “Fourier transform infrared spectroscopy measurements of H_2O-broadened half-widths of CO_2 at 4.3 μmThis article is part of a Special Issue on Spectroscopy at the University of New Brunswick in honour of Colan Linton and Ron Lees.,” *Can. J. Phys.*, vol. 87, no. 5, pp. 469–484, May 2009.
[43] D. A. Long, K. Bielska, D. Lisak, D. K. Havey, M. Okumura, C. E. Miller, and J. T. Hodges, “The air-broadened, near-infrared CO_2 line shape in the spectrally isolated regime: Evidence of simultaneous Dicke narrowing and speed dependence,” *J. Chem. Phys.*, vol. 135, no. 6, p. 064308, Aug. 2011.
[44] L. Kuai, D. Wunch, R.-L. Shia, B. Connor, C. Miller, and Y. Yung, “Vertically constrained CO_2 retrievals from TCCON measurements,” *J. Quant. Spectrosc. Radiat. Transf.*, vol. 113, no. 14, pp. 1753–1761, Sep. 2012.
[45] Conner et al., “An experimental algorithm for Vertical Profile Retrieval from TCCON Near IR Spectra.,” *Atmos Meas Tech*, 2015.
[46] Dohe, S., *Measurements of atmospheric CO_2 columns using ground-based FTIR spectra.* 2013.

Figures

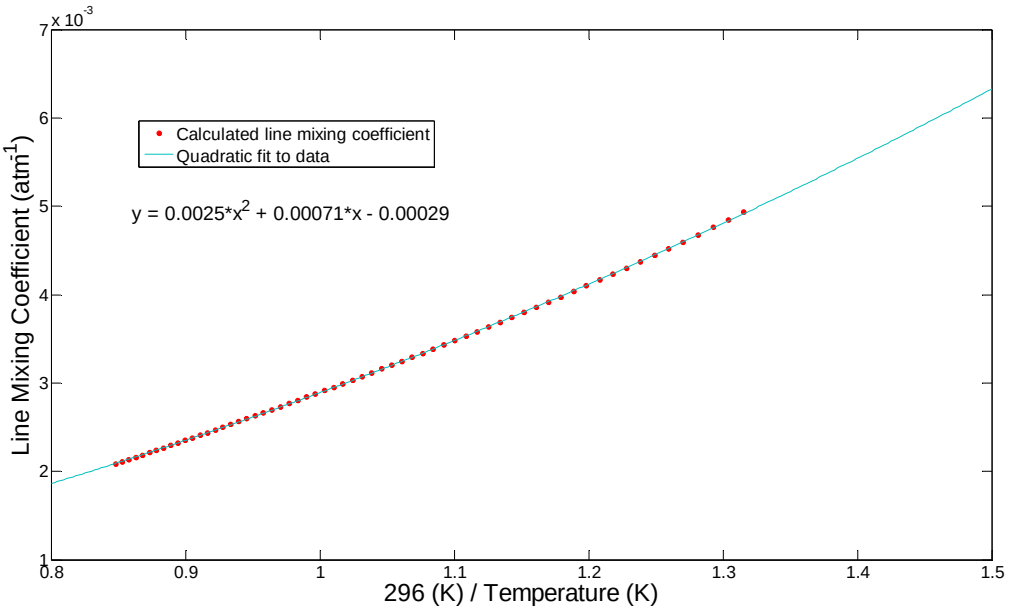

Figure 1: Temperature dependence of the P(24) line mixing coefficient calculated using spectroscopic parameters from Devi et al. Ref. [8]. A quadratic line is fitted to the data, and the coefficients of the line can be used to calculate the line mixing coefficient at any given temperature.

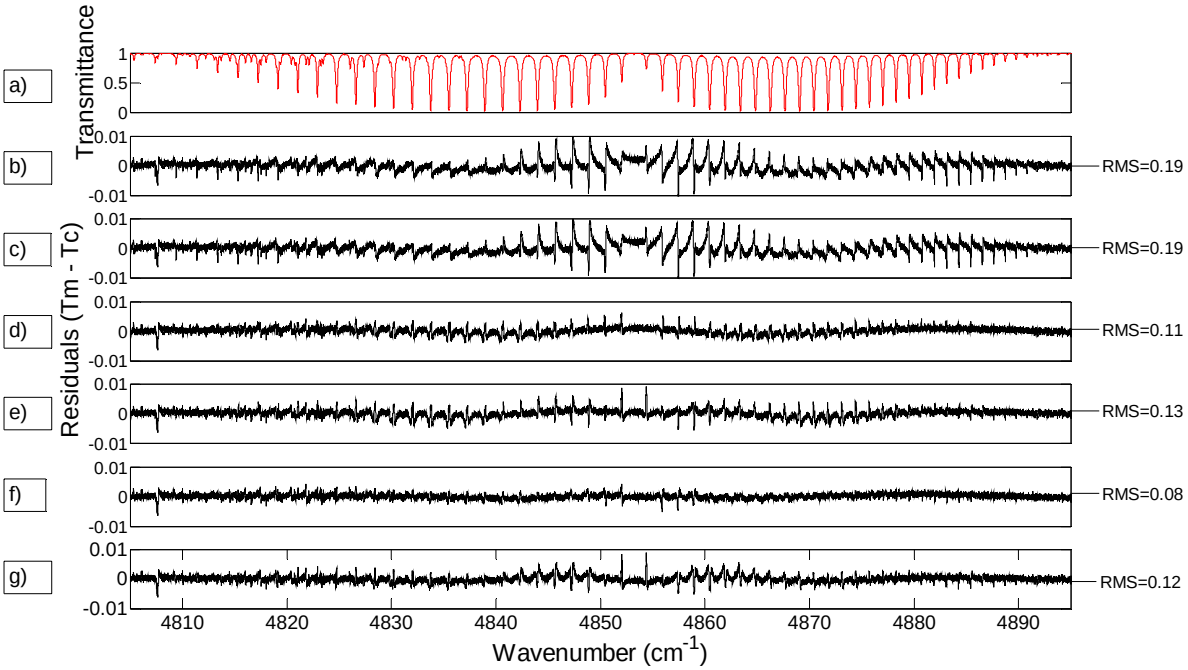

Figure 2: Panel (a) shows the laboratory spectrum of air-broadened CO_2 for the strong CO_2 band. The next six panels show the residuals (measured minus calculated spectra). (b) Voigt line shape with HITRAN 2008. (c) Voigt line shape with HITRAN 2012 parameters. (d) Voigt line shape with line mixing and HITRAN 2008. (e) Voigt line shape with line mixing and HITRAN 2012 parameters, with the air-broadened widths scaled by 0.985 and self-broadened widths scaled by 0.978. (f) qSDV+LM and HITRAN 2008 parameters, with air-broadened widths divided by 0.985 and self-broadened widths divided by 0.978. The same speed-dependent parameter $\alpha^i = 0.11$ is used for all lines. (g) qSDV+LM and HITRAN 2012 parameters and, $\alpha^i = 0.11$ for all lines.

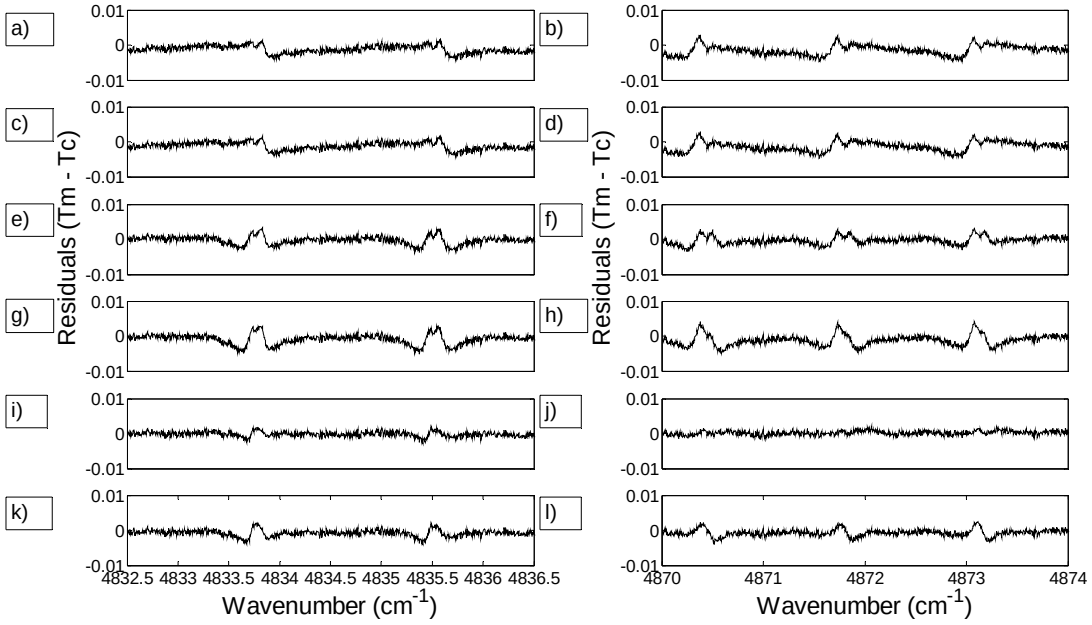

Figure 3: Same as Figure 2, showing details of the residualsfor P(24)-P(26) (panels a,c,e,g,i, and k) and R(22)-R(26) (panels b,d,f,h,j, and l).

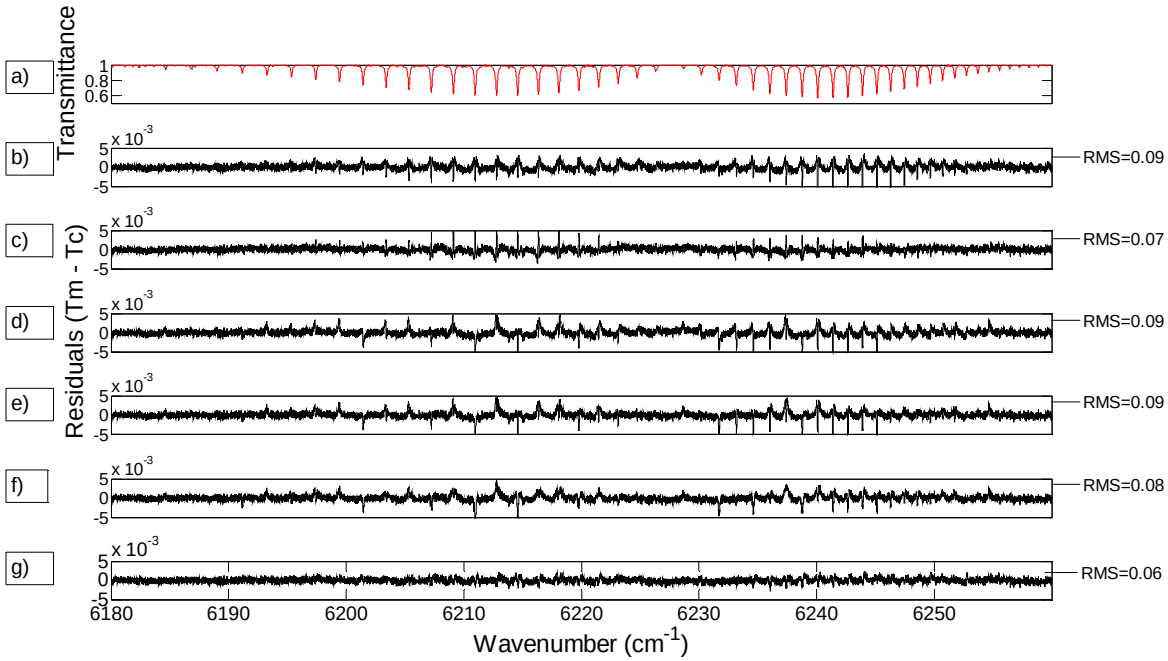

Figure 4: Panel (a) shows the measured laboratory spectrum for the weak CO_2 band 1. The next six panels show the residuals for a given set of spectroscopic parameters and a spectral line shape used to calulate the CO_2 absorption coefficients for the weak CO_2 band 1. (b) Voigt with atm.101 [25]. (c) Voigt with line mixing and atm.101 [25]. (d) Voigt with Predoi-Cross et al. (Ref. [10], [11], and [32]). (e) Voigt with line mixing and Predoi-Cross et al. (Ref. [10], [11], and [32]). (f) qSDV+LM and Predoi-Cross et al. (Ref. [10], [11], and [32]). (g) qSDV+LM and Devi et al. (Ref. [8]).

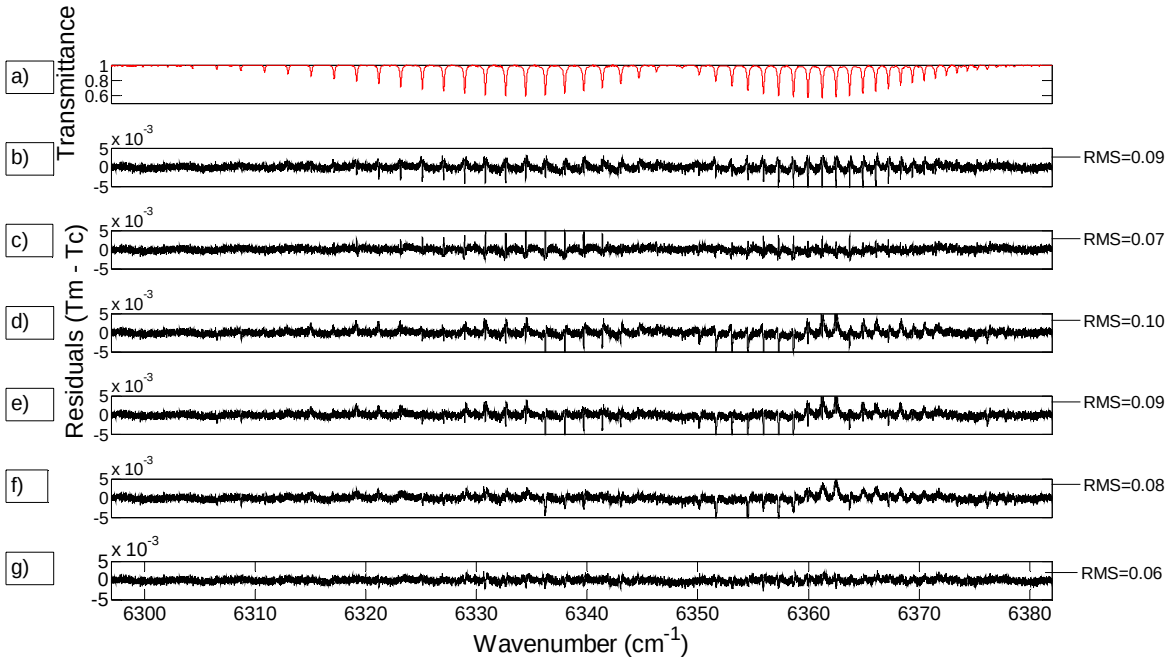

Figure 5: Same as Figure 4, but for absorption coefficients calculated for weak CO_2 band 2.

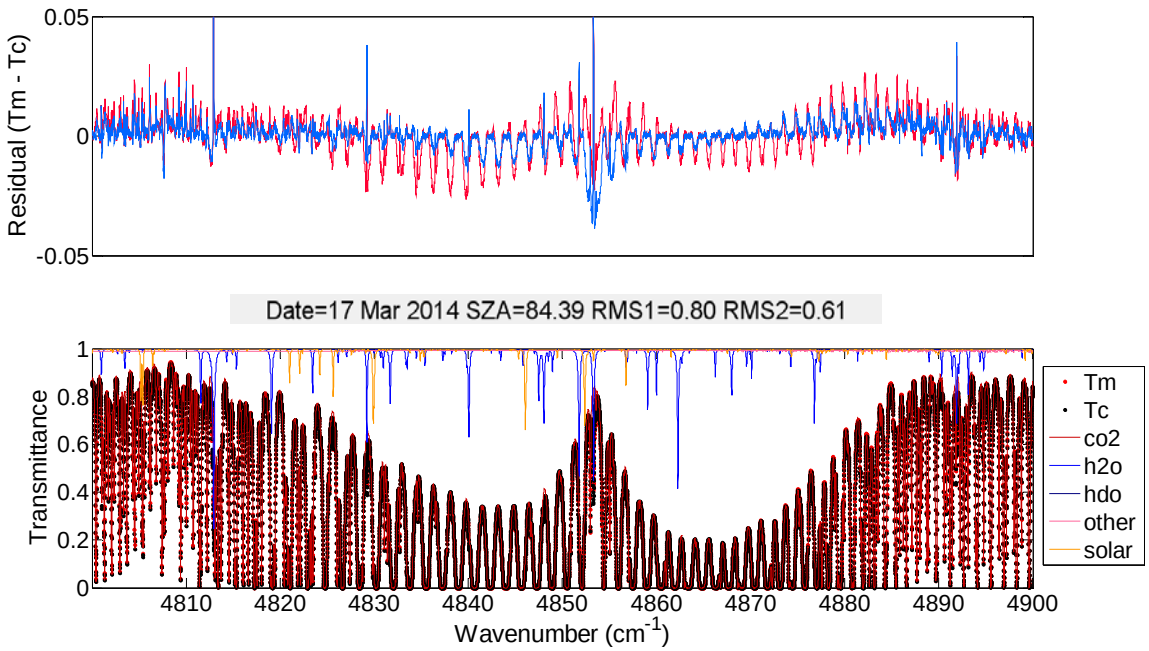

Figure 6: A typical Eureka spectrum recorded at a SZA of 84.39° on March 17, 2014 for the strong CO_2 band, as shown in red dots on the bottom panel. The calculated spectrum, using qSDV+LM, is shown with black dots and the contribution from all species follows the colour code of the legend on the right. The top panel shows the two residuals (measured minus calculated spectrum). The red line is the residual for CO_2 absorption coefficients caculated using HITRAN 2008 parameters with a Voigt line shape. The RMS for the red residual is 0.80% (RMS1 in plot). The blue line is the residual when CO_2 absorption coefficients are calculated using the adjusted HITRAN 2008 parameters with qSDV+LM. The corresponding RMS residual is 0.61% (RMS2 in plot).

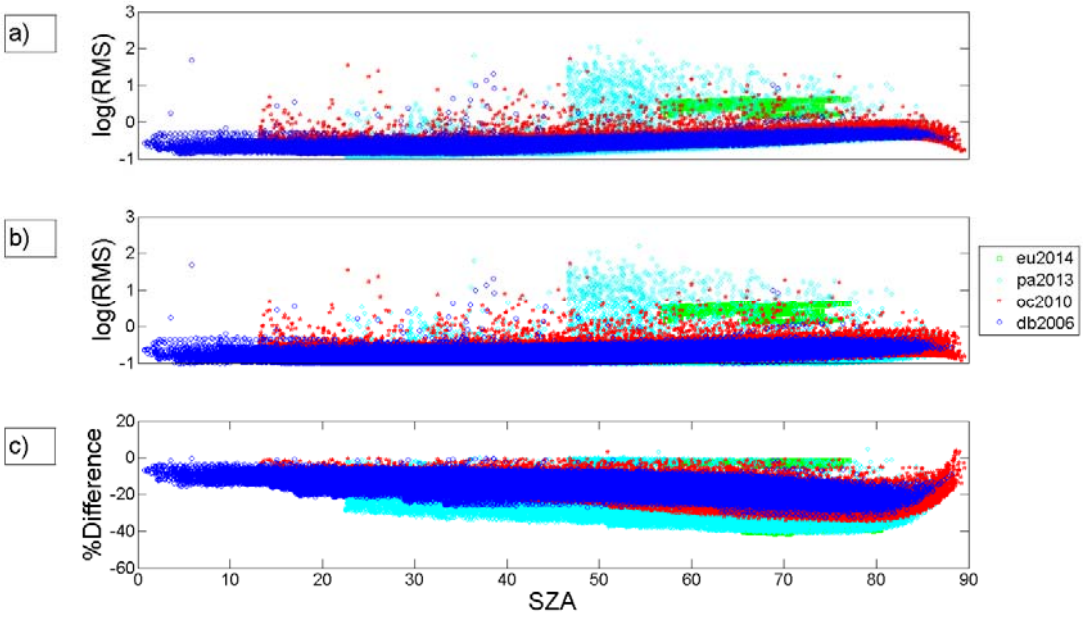

Figure 7: The RMS residual of solar spectra fitted with a Voigt (panel a) and qSDV+LM (panel b) spectral line shape for the strong CO_2 band as a function of SZA. The percent difference between the RMS residual obtained using the Voigt and qSDV+LM spectral line shapes is shown in panel c. Eureka measurements are in green, Park Falls in light blue, Lamont in red, and Darwin in dark blue.

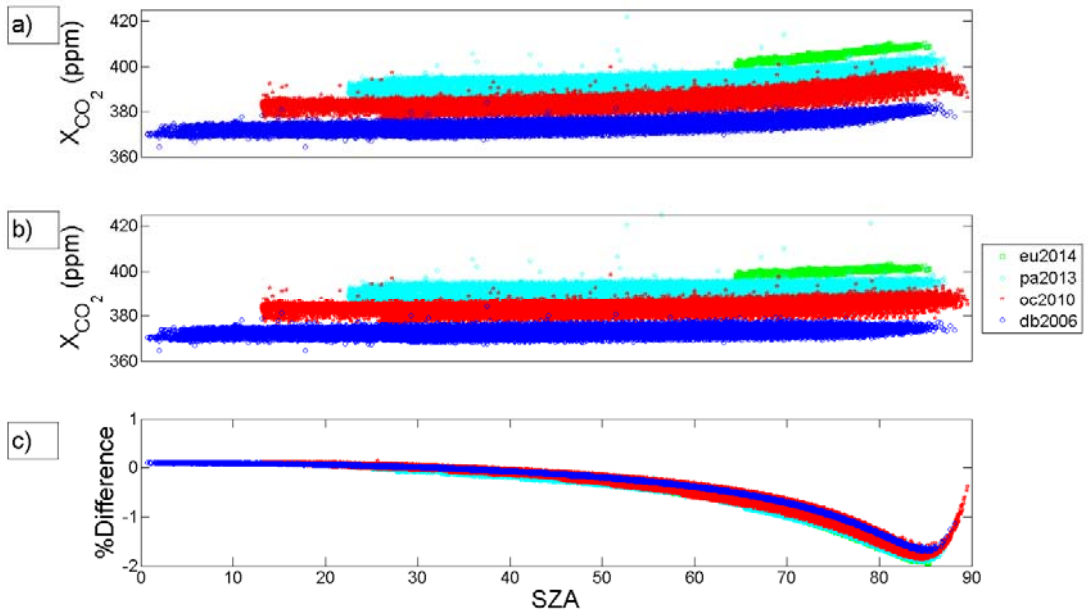

Figure 8: XCO_2 (using CO_2 column retrieved from the strong CO_2 band) plotted as a function of SZA. In panel a, XCO_2 was calculated using CO_2 column retrieved using a Voigt. Panel b, XCO_2 was calculated using CO2 column retrieved using a qSDV+LM. The percent difference $((XCO_2^{qSDV+LM} - XCO_2^{Voigt})/ XCO_2^{Voigt})x100$ is shown in panel c.

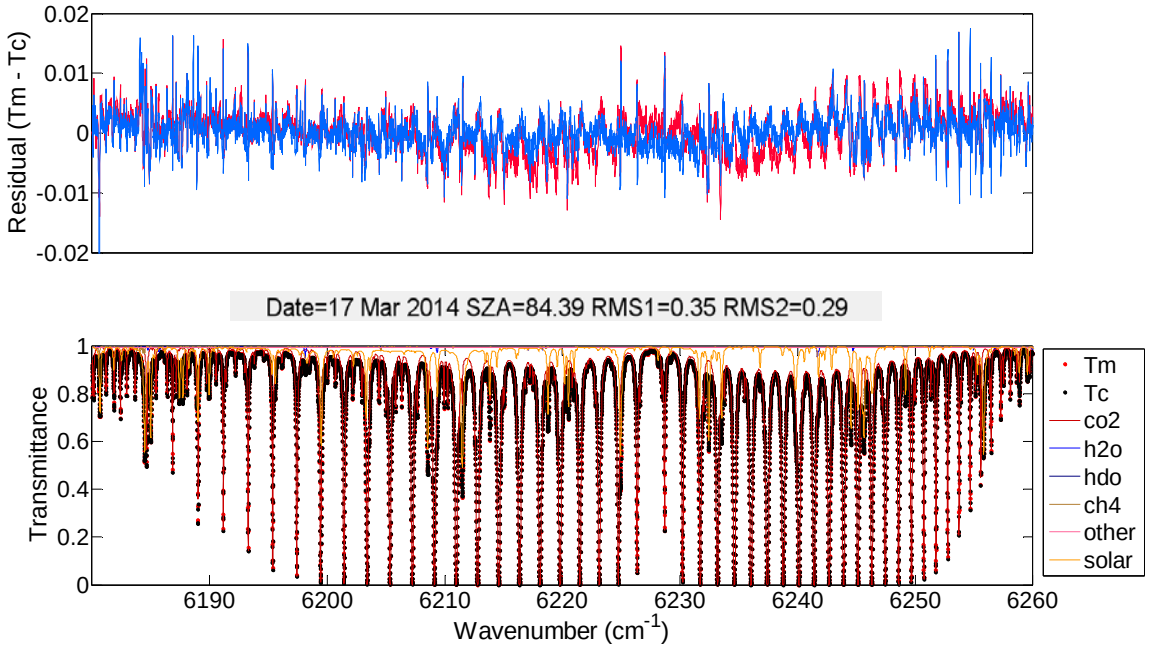

Figure 9: A Eureka spectrum recorded at a SZA of 84° on March 17, 2014 for the weak CO_2 band 1, as shown in red dots on the bottom panel. The calculated spectrum using, qSDV+LM, is shown with black dots and the contribution from all species follows the colour code of the legend on the right. The top panel shows the two residuals (measured minus calculated spectrum). The red line is the residual for CO_2 absorption coefficients caculated using Ref. [25] parameters with a Voigt line shape. The RMS for the red residual is0.35% (RMS1 in plot). The blue line is the residual using Ref. [8] parameters with qSDV+LM. The corresponding RMS residual is 0.29% (RMS2 in plot).

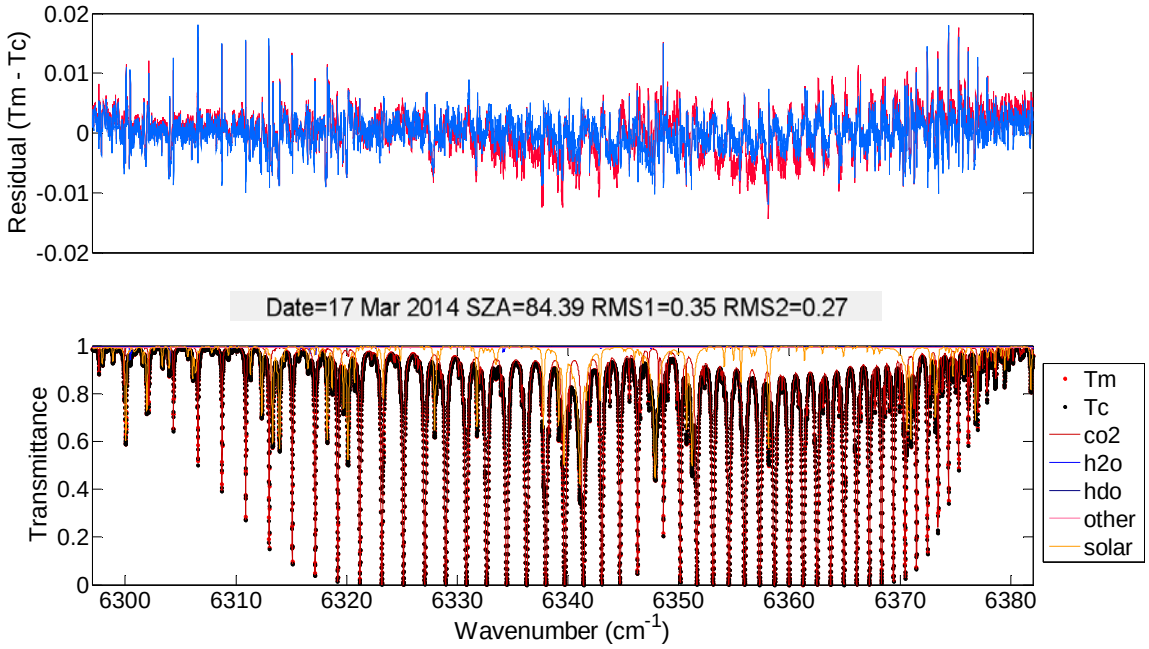

Figure 10: Same as Figure 9, but for the weak CO_2 band 2.

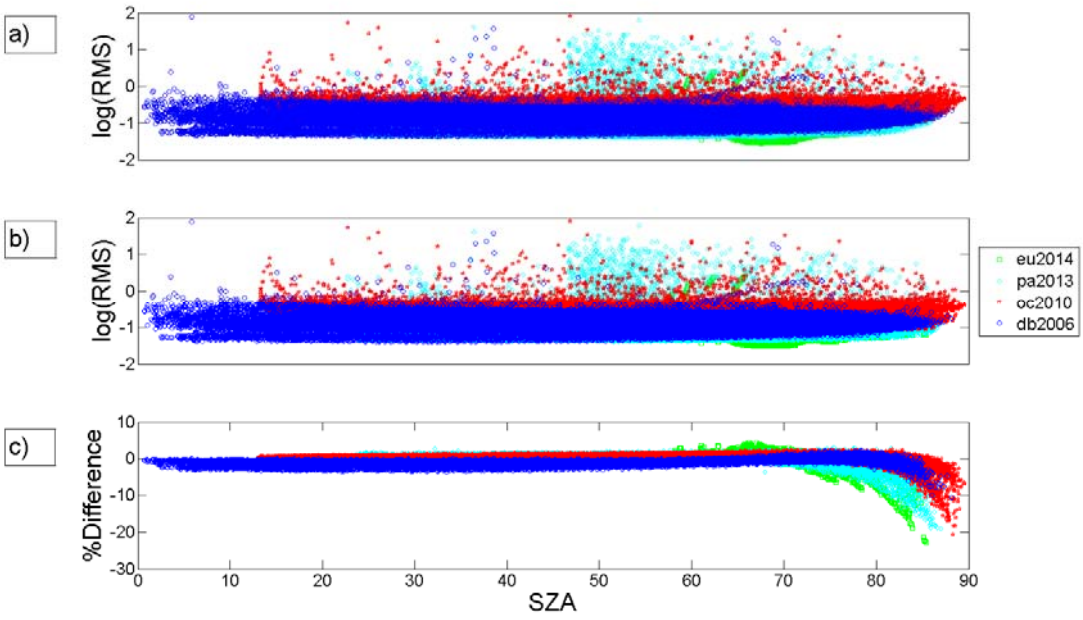

Figure 11: Same as Figure 7 except RMS residual is for the weak CO_2 band 1.

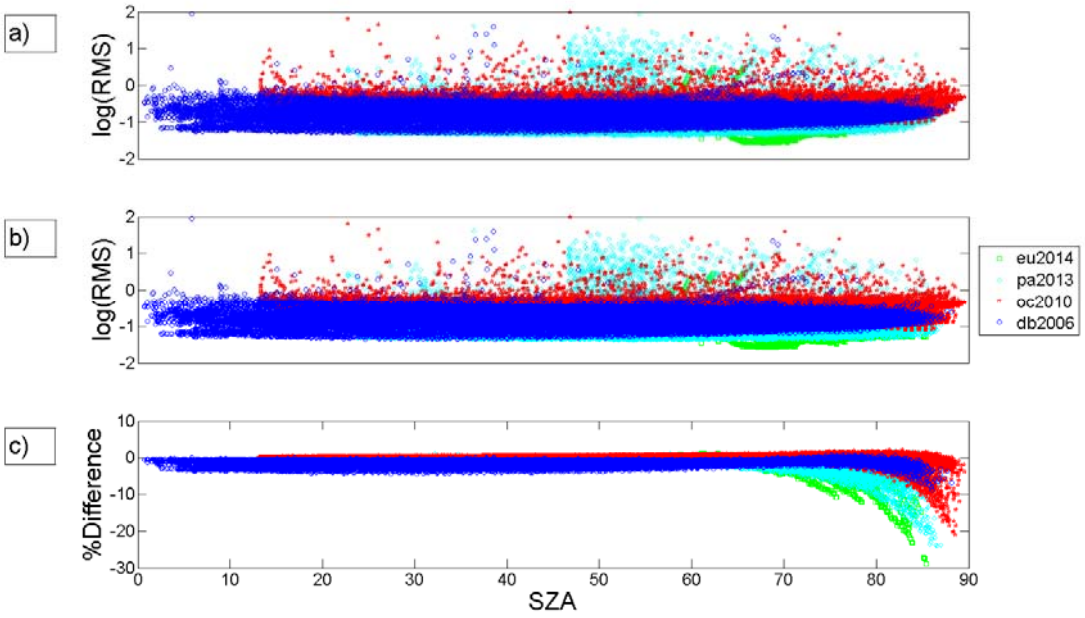

Figure 12: Same as Figure 7 except RMS is for the weak CO_2 band 2.

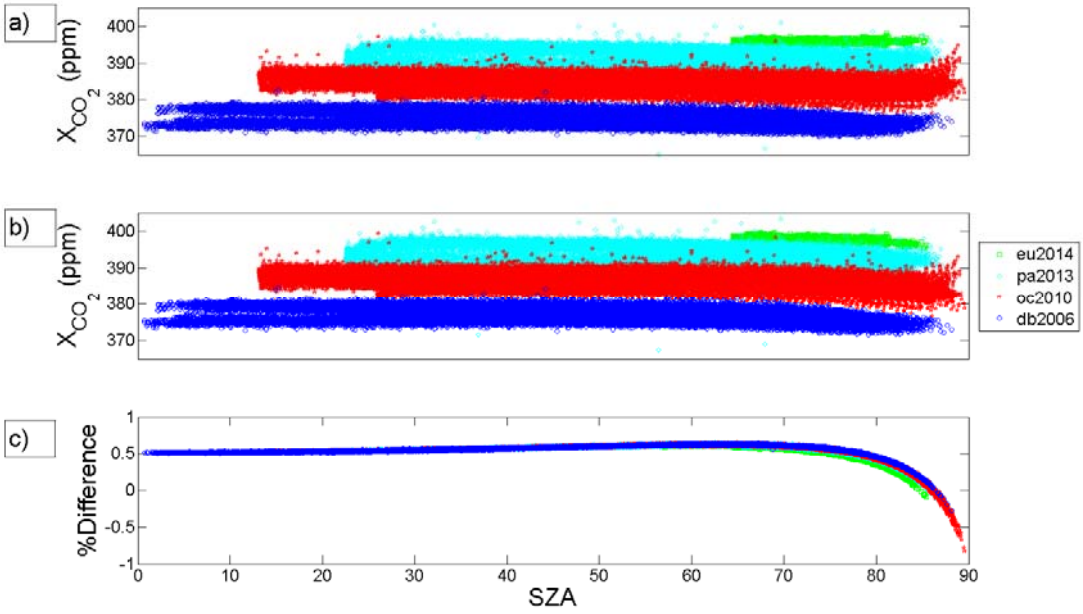

Figure 13: Same as Figure 8 except XCO_2 is calculated using CO_2 column retrieved from the weak CO_2 bands.

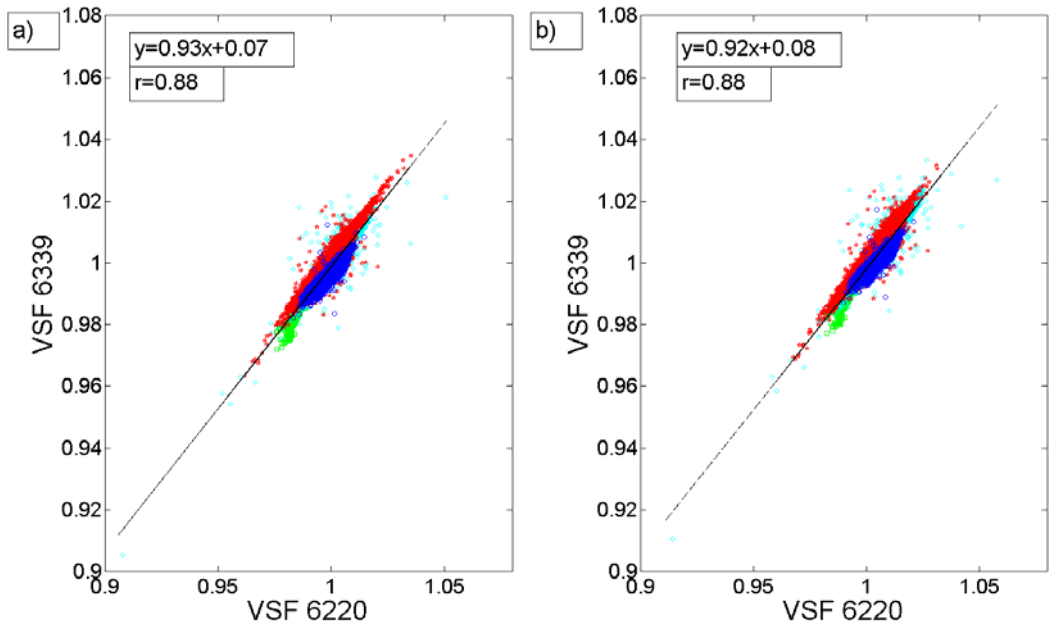

Figure 14: Correlations between the VSF retrieved using the weak CO_2 bands with the absorption coefficient calculated using: (a) the Voigt spectral line shape, (b) the qSDV+LM line shape.